IOSR Journal of Electronics and Communication Engineering (IOSR-JECE)
e-ISSN: 2278-2834,p- ISSN: 2278-8735.Volume 19, Issue 3, Ser. 1 (May. – June. 2024), PP 18-26
www.iosrjournals.org

Plant Cell Vacuolar Impedance And Equivalent Circuit

Koyu Chinen[1], Shoko Nakamoto[1], Ichiko Kinjo[2]
[1](Glex, Japan)
[2](National Institute Of Technology, Okinawa College, Japan)

Abstract:
We grated nine fruits and vegetables and filtered through a 20-micron paper filter to extract the plant cell vacuoles, and measured the S-parameters in the frequency range from 1 to 100 MHz. The primary equivalent circuit of the plant cell vacuole was a parallel circuit of resistance R and capacitance C. The value of R varied with the plant species, while the value of C was almost constant. Comparison with the equivalent circuit of NaCl solutions at different molar concentrations indicates that in plant cells, the resistance R is determined by the ion concentration in the plant vacuole and the capacitance C by the polar water molecules.
Key Word*: EIS; plant cell; vacuole; S-parameter; equivalent circuit; vegetable and fruit.*

Date of Submission: 04-04-2024 Date of Acceptance: 13-05-2024

I. Introduction

Electrochemical Impedance Spectroscopy (EIS), which measures electrical impedance and analyzes equivalent circuits and dielectric constants, has been widely studied because it provides valuable information for plant breeding, optimization of growing conditions, and disease control [1]– [12], [14] – [16]. Although impedance analyzers are mainly used for EIS measurements [12], [15], we have been studying the use of network analyzers, which allow the use of small probes in the high-frequency range [17].In plant impedance analysis, the cell membrane and wall play an essential role in the low-frequency range, and the vacuole plays an important role in the high-frequency range; the transition points can be clearly distinguished using the Smith chart and are known to vary depending on the plant samples [18]. When plant cells are classified by impedance, they comprise a cell wall consisting of a high-impedance part with high resistance, including cellulose, and a vacuole consisting of a low-impedance part that accounts for more than 70 % of plant cells. In this study, we focused on the low-impedance portion's vacuoles, extracted them from nine vegetables and fruits, measured the S-parameters, and analyzed their impedances.

II. S-Parameter Measurements Of Plant Samples Using A Portable VNA And A Small SMA Probe

When measuring the S-parameters using a small SMA probe for different plant surface geometries, the plant's skin may affect the measured values. Therefore, we measured the surface area where the skin was removed. The SMA probe consists of three pins: a central signal pin (gold-plated copper, 4 mm × φ 0.8 mm) surrounded by PTFE (polytetrafluoroethylene) and two ground pins (gold-plated brass, 4 mm × φ 0.8 mm) on the left and right sides, spaced 4 mm apart. Figure 1 shows a cross-sectional view of the SMA probe inserted into a plant sample with the skin removed. The reflection coefficient S_{11} of the S-parameter was measured in the frequency range from 1 to 100 MHz using a portable vector network analyzer (VNA) connected to the SMA probe. We obtained the reflection coefficient S_{11} of the S-parameter from the ratio of the transmitted signal voltage V^+ sent from the VNA to the plant sample and the reflected signal voltage V and calculated the impedance Z using a high-frequency circuit simulator AWR [19]. The SOLT (short, open, load, through) SMA terminal calibrated the measurement system. We verified the calibration by measuring and comparing the resistance of a 1608(mm) size 100 Ω SMD (surface-mount device) soldered between the signal and ground pins of the SMA probe for measurement.

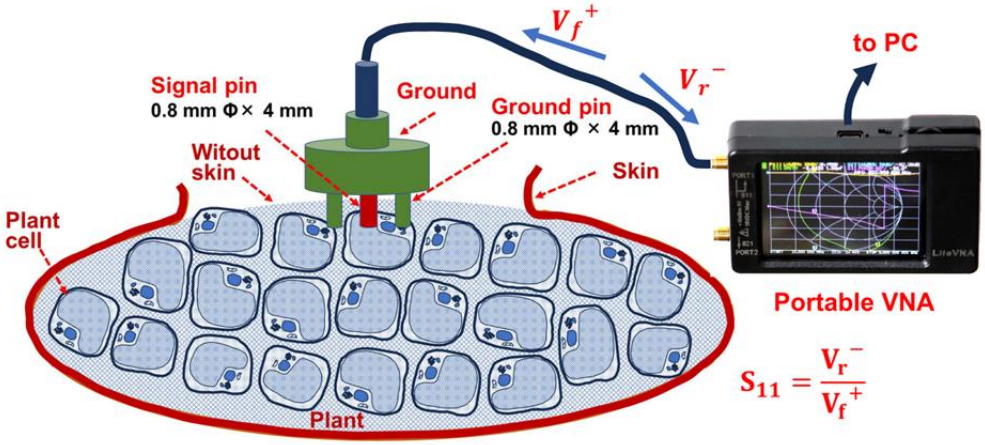

Figure 1: The reflection S-parameter S_{11} is measured in the frequency range from 1 to 100 MHz on the removed skin of a plant sample using a potable VNA and a small SMA probe.

III. Plant Sample Processing And Impedance Measurement Of Plant Cell Vacuole

We removed the skin and inserted the SMA probe into the surface of six plant samples. Then, we measured the S-parameter S_{11} and calculated the impedance *Z*. The results are shown in Figure 2. In the low-frequency range, the impedance differences between the plant samples were significant. The reflection coefficient S_{11} of the S-parameter measured by VNA is expressed in complex numbers or polar coordinates, so the input impedance *Z* of the measurement sample is represented by equations (1) and (2), where Z_0 is the characteristic impedance (usually 50Ω). The impedance is expressed in complex numbers $Z = Z\,(\mathrm{Re}) + Z\,(\mathrm{Im})$ or polar coordinates $Z = |Z| \angle\theta$. The S-parameter of plant samples was measured for the impedance of the vacuole, which accounts for more than 70 % of the plant cell, and the cell membrane and wall surrounding the cell [17]. Therefore, we grated the plant samples and filtered them using a 20-μm paper filter to extract the vacuole solutions, as shown in Figure 3.

$$Z = Z_0 \frac{1+S_{11}}{1-S_{11}} = Z_0 \frac{1+S_{11}(Re)+jS_{11}(Im)}{1-S_{11}(Re)-jS_{11}(Im)} = Z_0 = Z_0 \frac{\sqrt{\left(1+S_{11}(Re)\right)^2 + S_{11}(Im)^2}}{\sqrt{\left(1-S_{11}(Re)\right)^2 + S_{11}(Im)^2}} \varepsilon^{j(\theta_{11}-\theta_{12})} \tag{1}$$

$$\theta_{11} = tan^{-1} \frac{-S_{11}(Im)}{1-S_{11}(Re)} \qquad \theta_{12} = tan^{-1} \frac{S_{11}(Im)}{1+S_{11}(Re)} \tag{2}$$

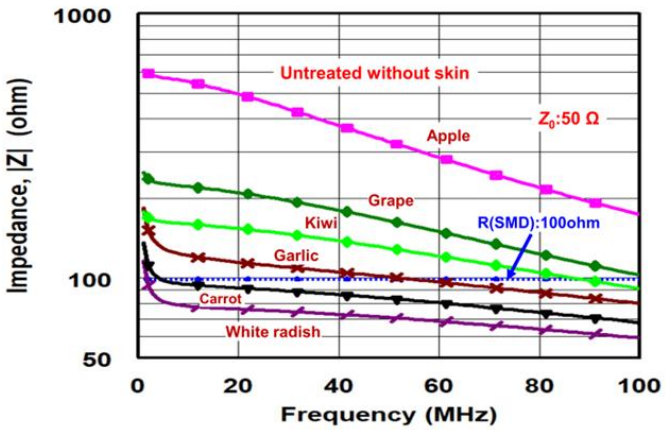

Figure 2: The skin was removed, and the SMA probe was inserted into the surface of six plant samples to measure the reflection S-parameter S_{11} and calculate the impedance *Z*. The measurement results of a 100 Ω SMD resistor for calibration confirmation are also shown.

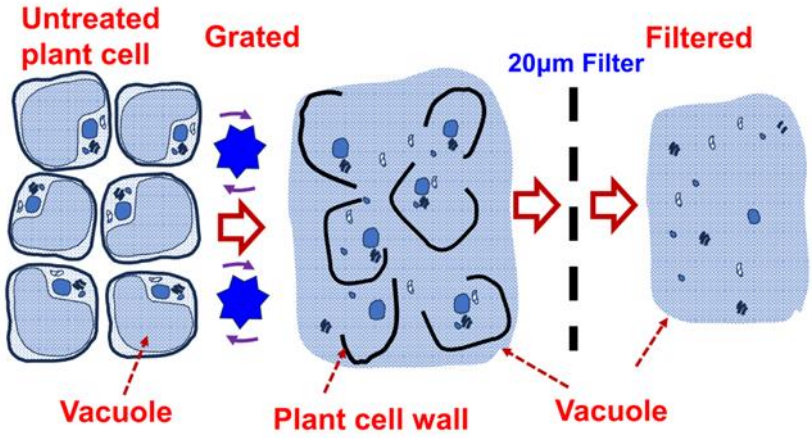

Figure 3: The plant sample was grated and filtered through a 20-μm paper filter to extract the solution in the vacuole.

We measured the reflection coefficients S_{11} of the S-parameters by inserting SMA probes into the peeled surfaces of three plant samples (tomato, grape, and garlic). Then, the S-parameters were measured for the solutions extracted by filtering with a 20-μm filter after grating the plant samples. The impedance Z calculated from the measured S-parameters S_{11} was plotted on the admittance grid of the Smith chart. The results are shown in Figure 4. To compare the plotted curves, the characteristic impedance was set to 100 Ω, and the measured data were recalculated with 100 Ω. The admittance grid was used because the measured vacuole impedance curves overlap with the admittance grid curves. In the impedance curves of the plant samples before the grating process, an overlapping area with the impedance grid curve appears in the low-frequency range (1 to several tens of MHz). This part is related to the cell wall and disappears when the sample is grated and filtered through a 20-μm filter [18]. A 20-μm filter removed the cell walls; most of the filtered solution contained the vacuole. The measured impedance of the vacuole solution decreased significantly, and the admittance's conductance G(S) ($Y = G + jB$) increased significantly.

IV. Synthesis Of Equivalent Circuits Of Plant Cells And Vacuoles

We synthesized the equivalent circuit of the vacuole by curve fitting with the measured values plotted on the admittance curve of the Smith chart. The equivalent circuit with a parallel capacitance C_1 and resistance R_2 was synthesized by superimposing the impedance curves on the admittance grid (see Figure 5). For comparison, the equivalent circuit of an untreated plant cell is shown. The equivalent circuits of untreated plant cells consist of series-parallel circuits and exhibit impedance characteristics that overlap the impedance grid in the low-frequency range and the admittance grid in the high-frequency range. A transition point of the impedance curve is revealed for garlic, as shown in Figure 4 [17], [18]. From the equivalent circuit of the synthesized vacuole, the impedance Z can be calculated using Kirchhoff's law. Equations (3) and (4) show the calculation formulas. The impedance Z calculated from the S-parameter S_{11} measurement of the vacuoles extracted through a 20-μm filter after grating the plant sample is plotted on a Smith Chart admittance chart.

$$Z = R_3 + \frac{K_1(\cos\theta_1 + \frac{1}{R_2}K_1)}{K_2} - j\frac{K_1 \sin\theta_1}{K_2} \tag{3}$$

$$K_1 = \sqrt{{R_1}^2 + \left(\frac{1}{\omega C_1}\right)^2} \qquad K_2 = (\cos\theta_1 + \frac{K_1}{R_2})^2 + (\sin\theta_1)^2 \tag{4}$$

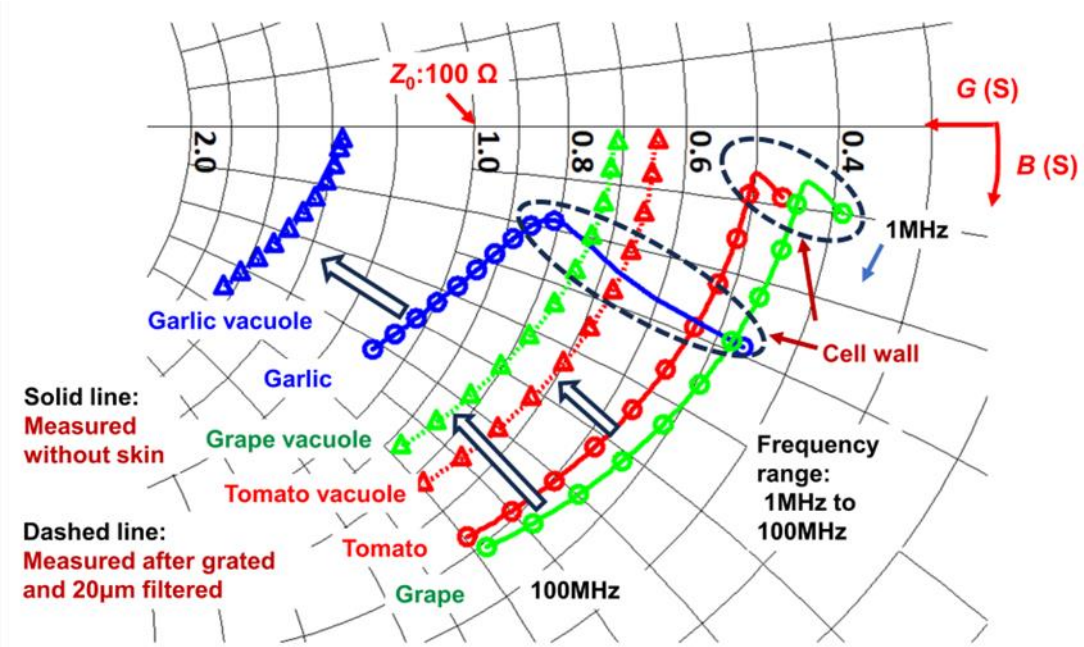

Figure 4: The impedance *Z* calculated from the reflection S-parameter S_{11} measurement of the vacuoles extracted through a 20-μm filter after grating the plant sample is plotted on a Smith chart admittance chart

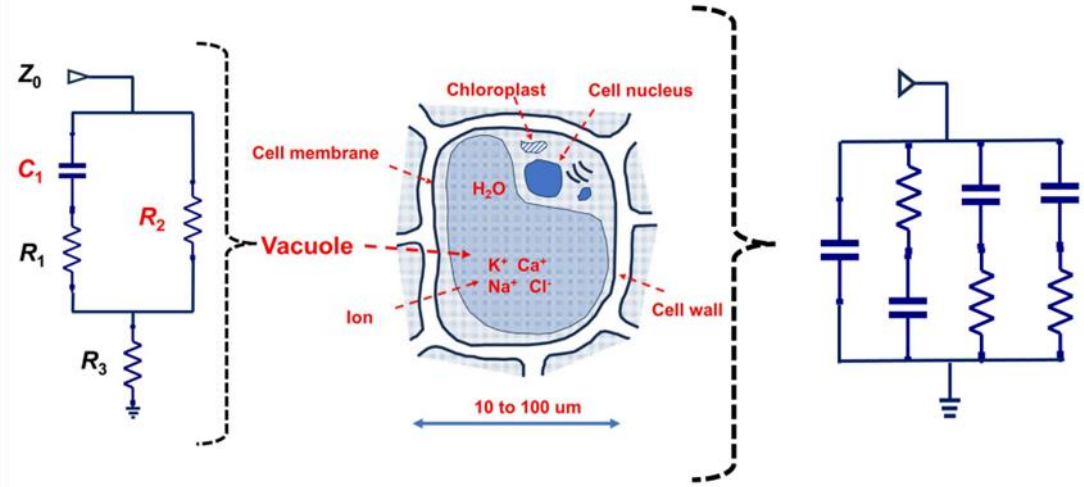

Figure 5: An equivalent circuit of a vacuole was synthesized from S-parameter measurements, considering the composition of plant cells, the ions, and polar water molecules contained in the vacuole

Figure 6 shows the measured impedance *Z* of solutions of vacuoles obtained from eight vegetables (white radish, potato, carrot, onion, cucumber, and tomato) and one fruit (apple) that were grated and filtered, the synthesized equivalent circuit, and the calculation results using equations (3) and (4). The measured and calculated values are almost coincidental. Table 1 lists the values of the components (C_1, R_1, R_2, R_3) of the synthesized equivalent circuit. For comparison with plant cell vacuoles, the measured values of four concentrations of NaCl ion solutions (0.1, 0.05, 0.025, and 0.001 mol/L) are plotted in Figure 6, and the calculated values using the equivalent circuit and equations (3) and (4) for the synthesized NaCl are shown [13]. Root vegetables have impedance values ranging between NaCl molar concentrations of 0.1 and 0.05 mol/L, vegetables between 0.05 and 0.025 mol/L, and fruits between 0.025 and 0.001 mol/L.

Table 1: Values for each of the four equipment circuit elements synthesized by reflection S-parameter S_{11} measurements for the nine plant samples.

Plants	C_1	R_1	R_2	R_3
Apple	12.5	4	274	7
Tomato	17	0	132	20

Grape	15.5	10	125	13
Cucumber	16.5	6	111	13
Onion	15.5	15	111	8
Kiwi	16.5	2	105	15
Carrot	22.5	0	69	25
Potato	20.0	16	61	16
White rdish	22.0	10	52	18
Unit	pF	Ω	Ω	Ω

V. Relationship Between The Impedance Of Plant Samples And The Components Of The Vacuole Equivalent Circuit

In the synthesized equivalent circuits of the vacuole for each of the nine vegetables and fruits, the resistance R_2 varies significantly, as shown in Figure 7. The changes in resistance Z (Re) = R of impedance Z (R + j X) and conductance G of admittance Y (G + j B) shown in Figure 6 are mainly related to the resistance R_2. In Figure 7, the differences in capacitance C_1 between the different types of vegetables and fruits are minor.

Table 2: Four element values of equivalent circuits synthesized by reflections parameter S_{11} measurements of NaCl solutions with different molar concentrations.

Solutions	C_1	R_1	R_2	R_3
Purewater	10	0	6438000	3
NaCl 0.001 mol/L	12	0	4327	1
NaCl 0.01 mol/L	13	0	546	8
NaCl 0.025 mol/L	14	0	189	15
NaCl 0.05 mol/L	17	5	93	17
NaCl 0.1 mol/L	26	9	40	18
Unit	pF	Ω	Ω	Ω

Table 2 shows the components (C_1, R_1, R_2, R_3) of the synthesized equivalent circuit for aqueous NaCl solutions. The value of resistance R_2 changes significantly with the molar concentration M. Figure 8 compares the relationship between R_2 and C_1 and the molar concentration M of NaCl solution on a logarithmic scale. The NaCl molar concentration M and the resistance R_2 are almost inversely proportional ($R_2 \cong 4.5/\mathrm{M}$). The characteristics of the impedance Z of the plant cell vacuole are similar to those of the impedance Z of the NaCl solution. The variation of the resistance R_2 in the synthesized equivalent circuit shows a strong correlation between the type of plant species and the molar concentration M of NaCl. The difference in resistance R_2 between solutions is due to the difference in the molar concentration M of NaCl. For the capacitance C_2, the correlation between the type of plant and the change in the molar concentration M of NaCl is small and almost constant. However, when the molar concentration M of NaCl exceeds 0.1, the friction between the hydrated ions increases, and the equivalent circuit and the relationship between the resistance R_2 and the molar concentration M deviate from the straight line shown in Figure 8.

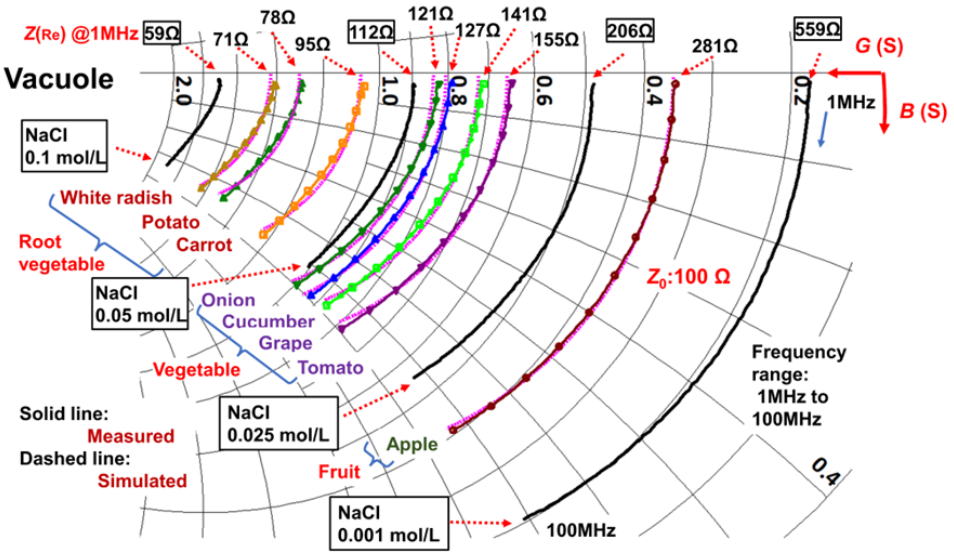

Figure 6: Comparison of impedance Z values calculated from reflection S-parameter S_{11} measurements for eight different vegetable and fruit vacuoles and four different concentrations of NaCl ionic water on a Smith chart.

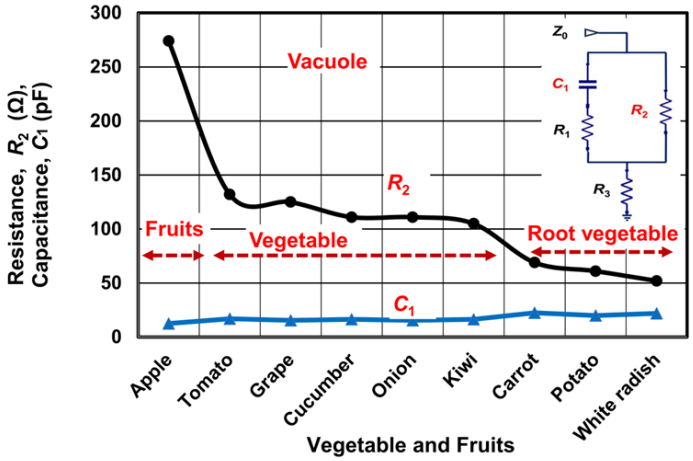

Figure 7: The resistance R_2 and the capacitance C_1 of the equivalent circuit elements of the vacuole for nine vegetables and fruits.

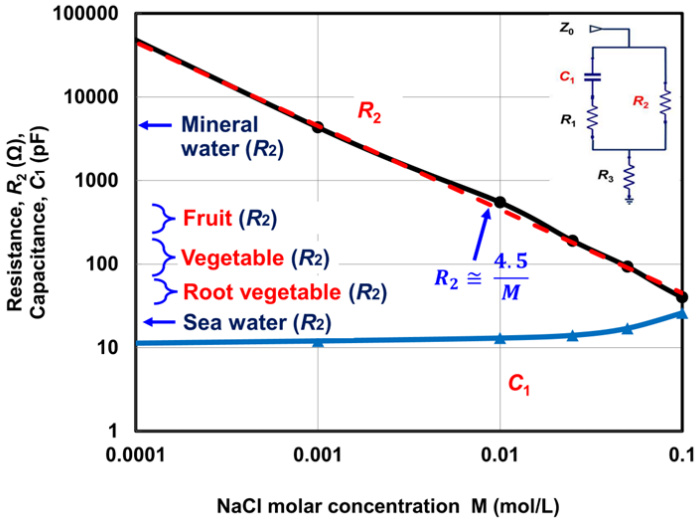

Figure 8: Change in resistance R_2 and capacitance C_1 of equivalent circuit elements synthesized from reflection S-parameter S_{11} measurements for NaCl solutions of different concentrations.

VI. Relationship Between Vacuolar And Environmental Water Impedances

Because environmental waters have a large impedance, we set the characteristic impedance Z_0 to 2500 Ω, converted the measured data to 2500 Ω, and plotted them on a Smith chart, as shown in Figure 9. The river and pond water samples were collected from the lower reaches of a 42.5 km-long river and from a pond in a park, which is close to a residential area but has a relatively large fish population. A city supplies the tap water. Rain water is the source of mineral water and has the highest impedance *Z*.

The measured impedance *Z* of the environmental water is enormous compared to the impedance of the vacuoles of the vegetables and fruits. Hence, the relationship between the environmental waters and the vacuoles of the vegetables and fruits is low. Table 3 shows the values of the elements that make up the synthesized equivalent circuit for environmental water. The values of resistance R_2 of the environmental water and the vacuoles of fruits and vegetables have a low correlation. The small value of C_1 has little effect on the value of impedance *Z*. Normal Saline solution (0.9 % NaCl, 0.15 mol/L), an aqueous solution with low impedance, was compared with the vacuoles of root vegetables (radish, potato, carrot) with low impedance *Z* (see Figure 10). The characteristic impedance Z_0 on the Smith chart is set to 50 Ω for a clear comparison. The minimum value of resistance R_2 for root vegetables is 52 Ω for white radish, but since R_3 is 18 Ω, the resistance value is effectively 70 Ω. Since R_3 of normal saline solution is 0 Ω, white radish's resistance (R_2 + R_3) is about two times larger than that of saline solution. Therefore, root vegetables have a higher impedance *Z* than normal saline. Figure 11 shows a schematic comparison of the impedance of environmental waters and plants. The impedance *Z* of seawater is the measured value for samples collected at the port, which is relatively high due to the influence of brackish

water. Most liquids filtered through a 20-μm paper filter after grating the plant samples are vacuoles. The ionized ions and water in the vacuole are the electrical resistance of the high-frequency signal (see Figure 12). The cations in the vacuole are K^+, Ca^+, and Mg^{2+}, and the anions are NO^-, Cl^-, NO_3^-, SO_4^-, PO_4^{3-}. The majority cation is K^+. Since water molecules are highly polar and rotate and vibrate in response to changes in high-frequency signals, they are treated as polar molecules in the frequency range of this study (1 to 100 MHz) [20]. In addition, hydrogen atoms can dissociate under high-frequency conditions and move around alone as the proton H^+. Polar water molecules assemble around a cation to form a hydrated ion, and the cation rarely moves around alone. The composition of ionized ions and polar water molecules in the vacuole is almost identical to that of an aqueous NaCl solution. Therefore, the vacuole's impedance characteristics can be compared to the NaCl solution [13]. In addition, the vacuole's equivalent circuit is highly similar to that of the NaCl solution. Low-impedance root vegetables have a high concentration of ions, fruits have a low concentration of ions, and vegetables are in between. Most environmental waters (rainwater, river water, pond water, mineral water, etc.) have a low ion concentration and a high impedance, which is not well related to the ion concentration in the vacuole of the plant cells. The polar water molecule H_2O is related to the capacitance C_1 in the equivalent circuit; it determines the susceptance component $B = j\omega C$ of the admittance Y of most water-containing substances. Thus, the capacitance C_1 for water-containing vegetables, fruits, salt water, and environmental water is due to polar water molecules and has almost the exact value of 10 to 20 pF. The resistance R_3 is a parameter that complements the resistance R_2 at low measurement frequencies, and the impedance can be thought of as ($R_2 + R_3$).

VII. Relationship Between Ionized Ions And Vacuole Impedance

We grated plant samples and filtered using a 20-μm paper filter to extract the vacuolar solution to analyze the impedance Z of vacuoles, which constitute more than 70 %of plant cells. We measured the reflection coefficient S_{11} of the S-parameter of the vacuole in the range from 1 to 100 MHz using a portable VNA and a small SMA probe and calculated the impedance Z from S_{11}. We plotted the impedance Z on the admittance grid of a Smith chart and synthesized an equivalent circuit by curve fitting. The main components of the equivalent circuit were resistance R_2 and capacitance C_1, connected in parallel. The value of resistance R_2 varied depending on the type of plant species and became larger for root vegetables, vegetables, and fruits, in that order. The capacitance C_1 was almost constant. We measured the impedance Z and synthesized the equivalent circuit for the NaCl solution. The resistance R_2 of the synthesized circuit of NaCl solution varied inversely with the molar concentration M, while the capacitance C_1 was almost constant. The plant cell vacuole and NaCl solution showed a high similarity in impedance characteristics and equivalent circuit structure. Therefore, the ionic concentration M and polar water molecules determine the impedance Z of plant vacuoles. The ionic concentration M determined the resistance R of the impedance Z, the conductance G of the admittance Y, and the polar water molecules determined the reactance jX and susceptance jB.

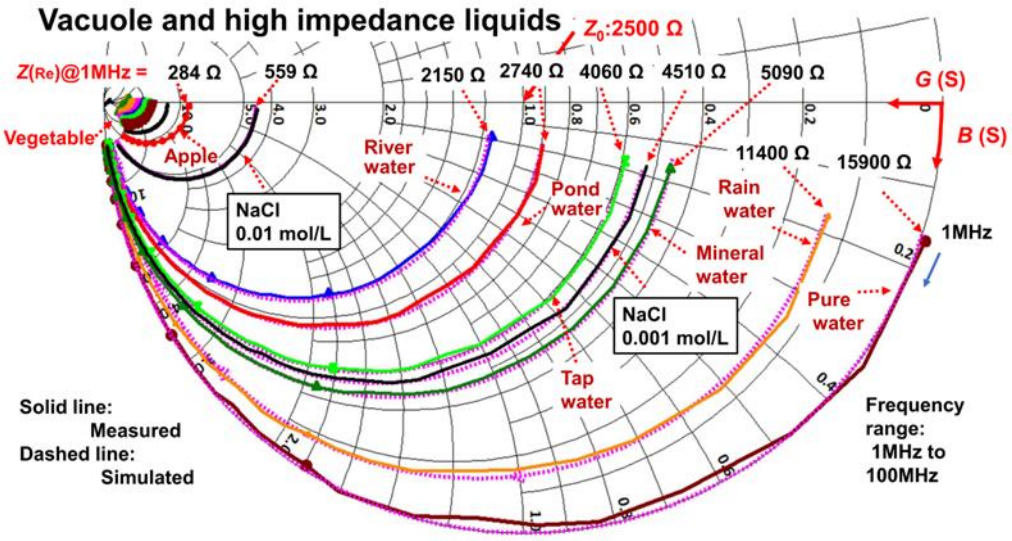

Figure 9: Comparison of the impedance Z values calculated from reflection S-parameter S_{11} measurements of vegetable and fruit vacuoles and environmental water on a Smith chart.

Table 3: Values of four elements of equivalent circuits synthesized from reflection S- parameter S_{11} measurements for environmental water.

Water	C_1	R_1	R_2	R_3
Rain water	11.0	0	18510	23
Mineral water	12.0	0	4327	1
Tap water	10.0	0	4217	4
Pond water	11.5	0	2778	9
River water	13.5	0	1826	5
Unit	pF	Ω	Ω	Ω

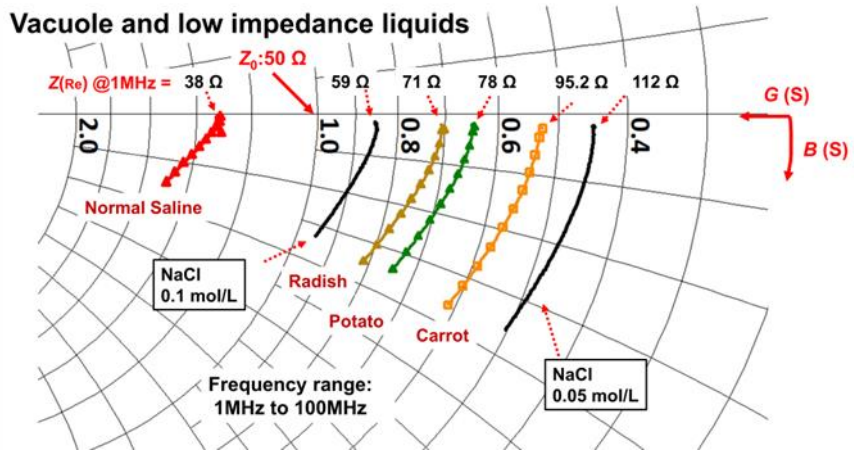

Figure 10: Comparison of the impedance Z values calculated by measuring the reflection S-parameter S_{11} for low-impedance vegetable and fruit vacuoles and normal saline solutions on a Smith chart.

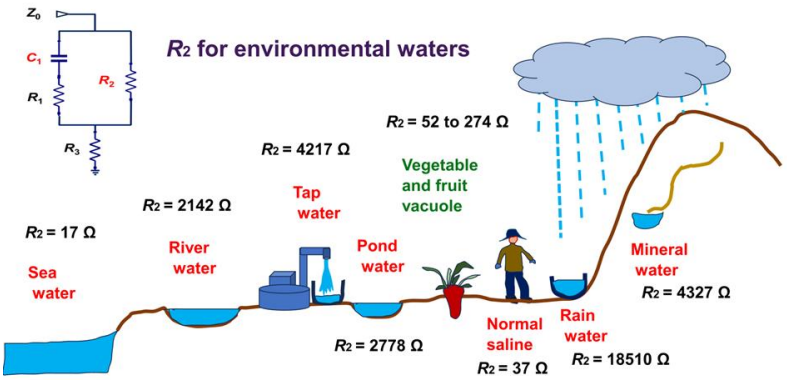

Figure 11: Comparison of resistance R_2 of the equivalent circuits for environ mental waters.

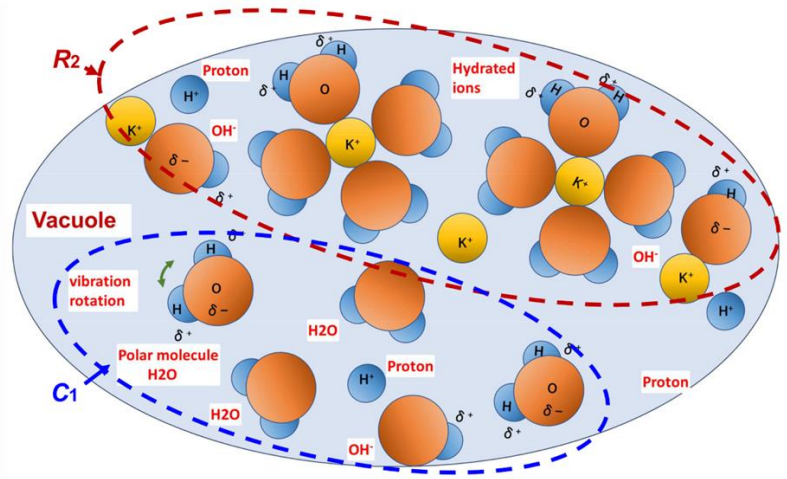

Figure 12: Ionized ions, polar water molecules, protons, and hydrated ion molecules in plant cell vacuoles.

VIII. Conclusions

We grated plant samples and filtered using a 20-μm paper filter to extract the vacuolar solution to analyze the impedance Z of vacuoles, which constitute more than 70 % of plant cells. We measured the reflection coefficient S_{11} of the S-parameter of the vacuole in the range from 1 to 100 MHz using a portable VNA and a small SMA probe and calculated the impedance Z from S_{11}. We plotted the impedance Z on the admittance grid of a Smith chart and synthesized an equivalent circuit by curve fitting. The main components of the equivalent circuit were resistance R_2 and capacitance C_1, connected in parallel. The value of resistance R_2 varied depending on the type of plant species and became larger for root vegetables, vegetables, and fruits, in that order. The capacitance C_1 was almost constant. We measured the impedance Z and synthesized the equivalent circuit for the NaCl solution. The resistance R_2 of the synthesized circuit of NaCl solution varied inversely with the molar concentration M, while the capacitance C_1 was almost constant. The plant cell vacuole and NaCl solution showed a high similarity in impedance characteristics and equivalent circuit structure. Therefore, the ionic concentration M and polar water molecules determine the impedance Z of plant vacuoles. The ionic concentration M determined the resistance R of the impedance Z, the conductance G of the admittance Y, and the polar water molecules determined the reactance jX and susceptance jB.

References

[1]. A. Fuentes, J. L. Vzquez-Gutierrez, Maria B. Perez-Gago, E. Vonasek, N. Nitin, D. M. Barrett, "Application Of Non-Destructive Impedance Spectroscopy To Determination Of The Effect Of Temperature On Potato Microstructure And Texture", Journal Of Food Engineering, 133, Pp.16-22, (2014). Https://Doi.Org/10.1016/J.Jfoodeng.(2014).02.016

[2]. D. E. Khaled, N. Novas, J. A. Gazquez, R. M. Garcia, F. Manzano-Agugliaro, "Fruit And Vegetable Quality Assessment Via Dielectric Sensing", Sensors, 15, Pp.15363-15397, (2015). Https://Doi.Org/10.3390/S150715363

[3]. X. Zhao, Hong Zhuang, S. Yoon, Y. Dong, W. Wang, And W. Zhao, "Electrical Impedance Spectroscopy For Quality Assessment Of Meat, Fish: A Review On Basic Principles, Measurement Methods, And Recent Advances", Hindawi Journal Of Food Quality, 6370739, 16 Pages, (2017). Https://Doi.Org/10.1155/2017/6370739

[4]. B. M. Aboalnaga, L. A. Said, A. H. Madian, A. S. Elwakil, A. G. Radwan, "Cole Bio-Impedance Model Variations In Daucus Carota Sativus Under Heating And Freezing Conditions, "Ieee Open Access, Vol.7, Pp.113254-113263, (2019). Https://Doi.Org/10.1109/Access.(2019).2934322

[5]. I.Jocsak, G. Vegvari, E. Vozary, "Electrical Impedance Measurement On Plants: A Review With Some Insights To Other fields", Theor. Exp. Plant Physiol. 31:359-375, (2019). Https://Doi.Org/10.1007/S40626-019-00152-Y(0123456789)

[6]. R. Prakash, A. S. Ninan, R. G. Atkinson, R. J. Schaffer, I.C. Hallett, R. Schroder, "Fruit From Two Kiwifruit Geno-Types With Contrasting Softening Rates Show Differences In The Xyloglucan And Pectin Domains Of The Cell Wall, Christina G. Fullerton", Front. Plant Sci., Vol.11, (2020). Https://Doi.Org/10.3389/Fpls.2020.00964

[7]. S. Ehosioke, F. Nguyen, S. R, T. Kremer, E. Placencia- Gomez, J. A. Huisman, A. Kemna, M. Javaux, S. Garre, "Sensing The Electrical Properties Of Roots: A Review", Vadose Zone Journal, Vol. 19, Issue 1, E20082. (2020). Https://Doi.Org/10.1002/Vzj2.20082

[8]. M. R. Stoneman And V. Raicu, "Dielectric Spectroscopy Based Detection Of Specific And Nonspecific Cellular Mechanisms", Sensors, 21, 3177, Pp.1-24, (2021). Https://Doi.Org/10.3390/S21093177

[9]. Y. Liu, D. Li, J. Qian, B. Di, G. Zhang, And Z. Ren, "Electrical Impedance Spectroscopy (Eis) In Plant Roots Research: A Review", Plant Methods, 17:118, (2021). Https://Doi.Org/10.1186/S13007-021-00817-3

[10]. M. I. Hussain, A. El-Keblawy, N. Akhtar, A. S. Elwakil, Electrical Impedance Spectroscopy In Plant Biology", Sustainable Agriculture Reviews Vol.52, Pp. 395-416, (2021). Https://Doi.Org/10.1007/978-3-030-73245-5-12

[11]. M. Mohsen, L. A. Said, A. H. Madian, A. G. Radwan, A. S. Elwakil, "Fractional-Order Bio-Impedance Modeling For Interdisciplinary Applications: A Review", Ieee Access, Vol.9, Pp.33158-33168, (2021). Https://Doi.Org/10.1109/Access.2021.3059963

[12]. K. Kadan-Jamala, M. Sophocleousb, A. Jogc, D. Desaganic, O. Teig-Sussholzd, J. Georgioub, A. Avni, Y. Shacham-Diamand, "Electrical Impedance Spectroscopy Of Plant Cells In Aqueous Buffer Media Over A Wide Frequency Range Of 4 Hz To 20 Ghz", Method Article, Vol. 8, 101185, (2021). Https://Doi.Org/10.1016/J. Mex.2020.101185

[13]. K. Chinen, S. Nakamoto, I. Kinjo, "Two-Port Equivalent Circuit Deduced From S-Parameter Measurements Of Nacl Solutions," Iete Journal Of Research If 1.877, Pp.1- 9, (2022). Https://Doi.Org/10.1080/03772063.2022.2081264

[14]. J. C. Nouaze, J. H. Kim, G. R. Jeon, J. H. Kim, "Monitoring Of Indoor Farming Of Lettuce Leaves For 16 Hours Using Electrical Impedance Spectroscopy (Eis) And Double-Shell Model (Dsm)", Sensors, Vol. 22, Pp.9671, (2022). Https://Doi.Org/10.3390/S22249671

[15]. J. Cheng, P. Yu, Y. Huang, G. Zhang, C. Lu And X. Jiang, "Application Status And Prospect Of Impedance Spectroscopy In Agricultural Product Quality Detection", Agriculture 12, 1525. Pp.1-15, (2022). Https://Doi.Org/10.3390/Agriculture12101525

[16]. M. V. Haeverbeke, M. Stock, And B. D. Baets, "Equivalent Electrical Circuits And Their Use Across Electrochemical Impedance Spectroscopy Application Domaines", Ieee Access Vol. 10, Pp. 51363-51369, (2022). Https://Doi.Org/10.1109/Access.2022.3174067

[17]. K. Chinen, S. Nakamoto, I. Kinjo, "Rf Analysis Of Fruit And Vegetables Using Equivalent Circuits Deduced From S-Parameters", International Journal Of Electrical And Computer Engineering Research, Vol. 3, No. 2, Pp.18-24, (2023). Ttps://Doi.Org/10.53375/Ijecer.2023.342

[18]. K. Chinen And I. Kinjo, "A 3.5 Ghz Band Rf Wireless Signal Transmission Mechanism In Various Aqueous Solutions", Ssrg International Journal Of Electrical And Electronics Engineering, Vol.10, Iss.8, Pp102-111, (2023). Https://Doi.Org/10.14445/23488379/Ijeee-V10i8p110

[19]. Https://Www.Awr.Com

[20]. K. Chinen, S. Nakamoto, And I. Kinjo, "Relationship Between Impedance Transition Point And Cell Wall In Plant Tissue", Quest Journals, Journal Of Electronics And Communication Engineering Research, Vol.10, Iss.3, Pp. 09-18 (2024). Issn: 2321-5941